Supporting Information for:

The Influence of Aqueous versus Glassy Solvents on Protein Dynamics: Vibrational Echo Experiments and Molecular Dynamics Simulations

Aaron M. Massari[†], Ilya J. Finkelstein[†], Brian L. McClain[†], Anne Goj[#], Xin Wen[‡], Kara L. Bren[‡], Roger F. Loring[#], and Michael D. Fayer[†]

[†]Department of Chemistry
Stanford University, Stanford, CA 94305, USA

[‡]Department of Chemistry
University of Rochester, Rochester, NY 14627-0216

[#]Department of Chemistry and Chemical Biology
Baker Laboratory, Cornell University, Ithaca NY, 14853

email: fayer@stanford.edu

Aqueous Protein Sample Preparation

To prepare aqueous samples, lyophilized protein was dissolved in pH 7.0 D_2O phosphate buffer (50mM) to a concentration of 10-15 mM protein. The buffer pH was measured before addition of protein. The solutions were centrifuged at 14,000 rcf for 15 minutes to remove large particulates, after which the supernatant was removed and filtered through a 0.45 μm acetate filter (Pall Nanosep MF). The solutions were reduced with a 5-fold excess dithionite solution and stirred under a CO atmosphere for one hour. When necessary, the samples were further concentrated by centrifugation (Eppendorf 5415D) over modified polyethersulfone membranes (Pall Nanosep 10K Omega). The sample was then placed in a sample cell with CaF_2 windows and a 50 μm Teflon spacer. UV-visible (Varian Cary 3E) and FTIR (ATI Mattson Infinity 9495) absorption spectroscopies were performed to determine all protein concentrations. Typical aqueous

samples had mid-IR absorbances at the CO stretching frequency of 0.075 to 0.1 on a background absorbance of 0.35.

Spectrally-resolved Infrared Stimulated Vibrational Echo Experimental Setup

Tunable mid-IR pulses with a center frequency adjusted to match the center frequency of the protein sample of interest (1951 to 1976 cm^{-1}) were generated by an optical parametric amplifier pumped with a regeneratively amplified Ti:Sapphire laser. The bandwidth and pulse duration used in these experiments were 150 cm^{-1} and 100 fs, respectively. The mid-IR pulse was split into three temporally controlled pulses (~700 nJ/pulse). The delay between the first two pulses, τ, was scanned at each time T_w, the delay between pulses two and three. The three beams were crossed and focused at the sample. The spot sizes at the sample were ~150 μm. The vibrational echo pulse generated in the phase-matched direction was dispersed through a 0.5-meter monochromator and detected with either a liquid nitrogen-cooled HgCdTe array detector (Infrared Associates/Infrared Systems Development) or a liquid nitrogen-cooled InSb single element detector (EG&G Judson). The spectral resolution was 1.2 cm^{-1}. A power dependence study was performed on all samples and the data showed no power dependent effects.[1] Data collection for all samples was performed in an enclosed, dry air purged environment. For HbCO and H64V in trehalose, all linear and nonlinear spectroscopic data were collected in a chamber under 20 mTorr vacuum to ensure maximum dehydration. To confirm that the preparation procedure reproduced the samples studied in our previous work,[2,3] the H64V sample was also heated to 80 ^{o}C for ~24 hr under vacuum and then cooled to room temperature for data acquisition. The heating process

did not cause degradation of the film and did not change the protein's optical absorption spectra or vibrational echo decays (data not shown).

FFCF Extraction from Vibrational Echo Data

The static term in Eq. (1) contributes a Gaussian time decay to the dipole autocorrelation function and hence a Gaussian frequency contribution to the peak of the linear absorption spectrum. Since the two-pulse echo is designed to remove the effects of static line broadening, though this is in practice only true in the limit of massive static line broadening, the inclusion of the static term in Eq. (1) is expected to have a more significant effect on the absorption lineshape than on the vibrational echo.

Both substates in the aqueous HbCO data[4] were modeled with a bi-exponential FFCF (n = 2 in Eq. (1)). These two substates were constrained to have the same FFCF, with the ratio of the concentrations of the two substates used as an adjustable parameter. The blue substate (CIV) band[4] is necessary to reproduce the beats observed on the decays (see below).[5] The aqueous H64V and *Ht*-M61A and all three proteins in trehalose glasses were fit with a bi-exponential FFCF (n = 2 in Eq. (1)). Although the vibrational lifetime (T_1) for all three proteins is long enough to have only a small influence on the observed vibrational echo decays, it was included in the calculations to fit the experimental observables. The FFCF obtained from analysis of the data using response theory calculations is deemed correct when it can be used to calculate vibrational echo decays that fit the experimental vibrational echo data at all T_ws and simultaneously reproduce the linear absorption spectrum.

Computational Methods

The coupling constant λ in Eq. (2) has been measured by Boxer and coworkers with vibrational Stark spectroscopy for MbCO and other heme-CO systems, and has been found to be in the range λ=1.8-2.2 cm^{-1}/(MV/cm).[6] Our previous calculations for sperm whale myoglobin treated λ as an adjustable parameter, with an optimal value of $\lambda = 2.1$ cm^{-1}/(MV/cm) determined by simultaneous fitting of the absorption spectrum and stimulated vibrational echo. We have retained this optimal value of λ for all subsequent calculations for H64V.[7]

Our adoption of a model in which Coulombic forces drive vibrational frequency fluctuations is consistent with recent studies of nonlinear vibrational spectroscopy in molecular liquids that have demonstrated the validity of models based on electrostatic interactions.[8-11] For example, Moller and coworkers have shown that vibrational frequency fluctuations for the solute HOD in the solvent D_2O are dominated by electrostatic forces and are negligibly affected by short-range repulsive forces.[10] Since the local atomic density around the CO in the heme pocket is less than that of a dense fluid, we do not expect repulsive forces to contribute significantly to frequency fluctuations of the CO. Our electrostatic model has been validated by application to vibrational echo experiments in sperm whale MbCO in aqueous solution.[12]

Influence of the heme atoms on frequency fluctuations

Within the electric field model used here and for the force field employed in our simulations, interactions between the heme and the ligand do not contribute to $C(t)$ on

time scales relevant to the vibrational echo measurements.[12] The heme exerts a significant electric field on the CO, inducing a static vibrational frequency shift, but this field is nearly static on the time scale relevant to $C(t)$ in Fig. 6.

Spectroscopic substates and accidental degeneracy beats (ADBs) of HbCO

The aqueous HbCO spectrum (Fig. 1c) exhibits 2 maxima: The main band at 1951 cm^{-1} with a FWHM of 8.3 cm^{-1} and a smaller band at 1969 cm^{-1}. In aqueous HbCO, these have been designated the CIII and CIV peaks,[4] respectively, and correspond to two unique protein structural states. Analogous to the extensive work done on MbCO, these states arise from the orientation of the histidine distal to the heme plane.[12-14] The CIII peak has the imidazole ring of the histidine swung into the heme plane, whereas the imidazole ring is oriented out of the hydrophobic pocket surrounding the heme in the CIV structure.

Figure S1a shows the vibrational echo decays for HbCO at a single T_w (0.5 ps) in aqueous solution and a dry trehalose glass. The oscillations in the data occur at the frequency of the HbCO vibrational anharmonicity (25 cm^{-1}) and are attributed to an accidental degeneracy beat (ADB) between the CIII and CIV substates.[5,15] In HbCO, the 1-2 transition of the CIV transition (25 cm^{-1} red-shifted from the 0-1 transition frequency) overlaps spectrally with the 0-1 transition of the CIII subensemble. The relative amplitudes of the substates determine the magnitude of the beat. The ratio of the CIII to CIV substate concentrations is 10:1 and 10:3.3 in aqueous and trehalose environments, respectively. The low concentration of the CIV state in both solvents precludes the unambiguous acquisition of vibrational echo data at this frequency.[1,16,17]

It is apparent from Fig. S1a that the oscillations in the vibrational echo decays at the CIII maximum complicate interpretation of the data. The fitting procedure described in Sec. IIB allows us to "turn off" the CIV substate to examine the CIII vibrational echo decay without the influence of ADBs.[16] Once the FFCFs for both substates are determined by simultaneously fitting the linear spectrum and vibrational echo decays at all T_ws, the extracted $C(t)$ for CIII is used to calculate the vibrational echo decay without the influence of the CIV substate. Figure S1b (same as Fig. 2c, but on a linear scale) demonstrates the results of turning off the CIV ADBs.

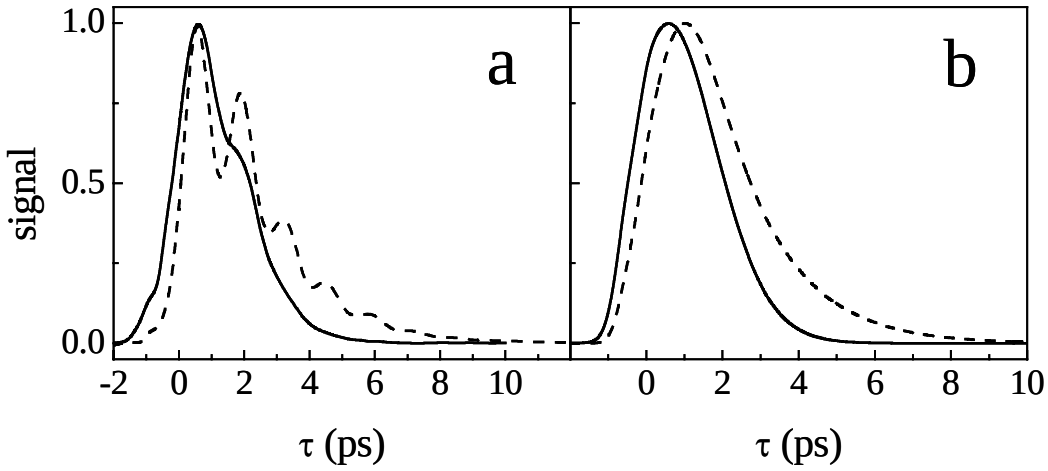

Figure S1a. a) Vibrational echo decays for HbCO at a single T_w (0.5 ps) in aqueous solution (solid line) and a dry trehalose glass (dashed line), and b) the same vibrational echo decays without ADBs from the CIV substate.

Spectral diffusion data for all proteins

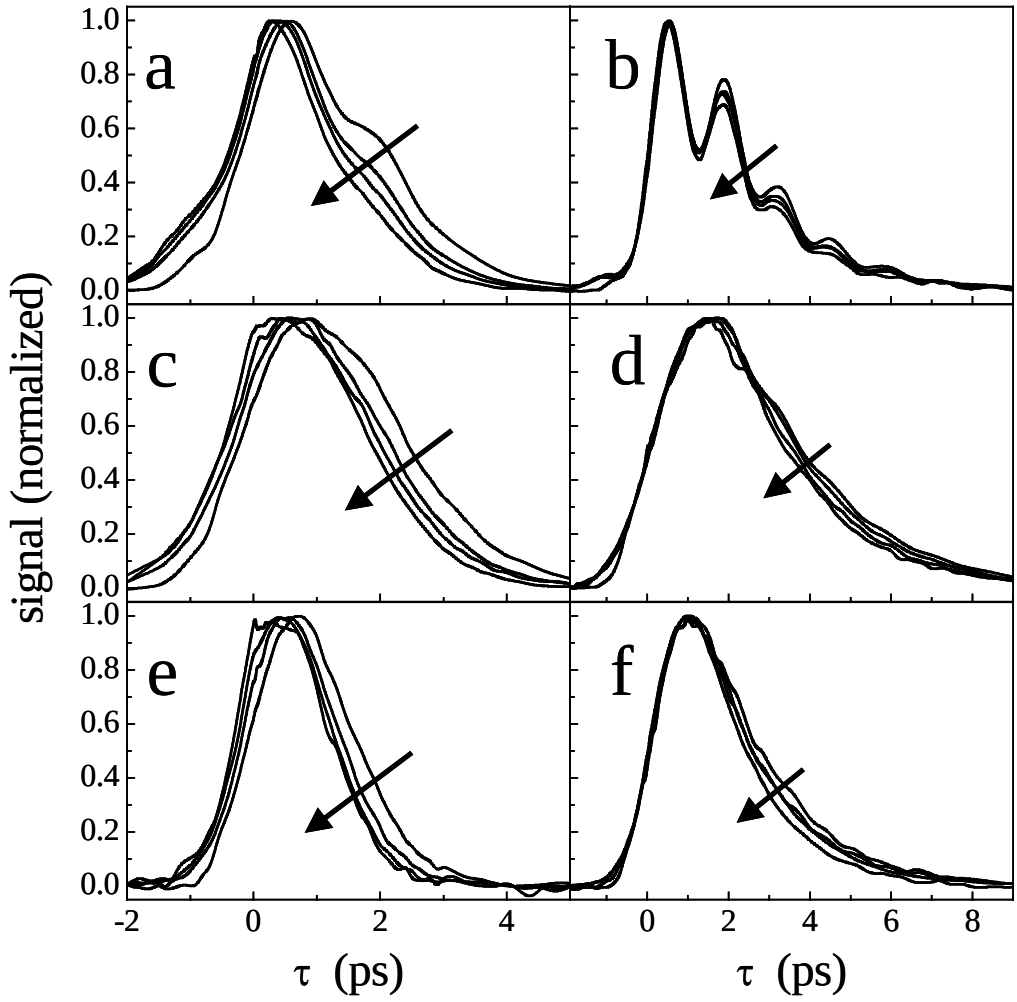

Figure S2. Vibrational echo decays as a function of T_w: a) HbCO in aqueous solution at 1951 cm^{-1}, b) HbCO in trehalose glass at 1954 cm^{-1}, c) H64V in aqueous solution at 1967 cm^{-1} (same as Fig. 3a), d) H64V in trehalose glass at 1971 cm^{-1} (same as Fig. 3b), e) *Ht*-M61A in aqueous solution at 1974.7 cm^{-1}, and f) *Ht*-M61A in trehalose glass at 1976 cm^{-1}. All plots show T_w = 0.5, 4, 8, and 16 ps and the arrows indicate the direction of vibrational echo decay shifting with increasing T_w.

Nonlinear response theory fitting

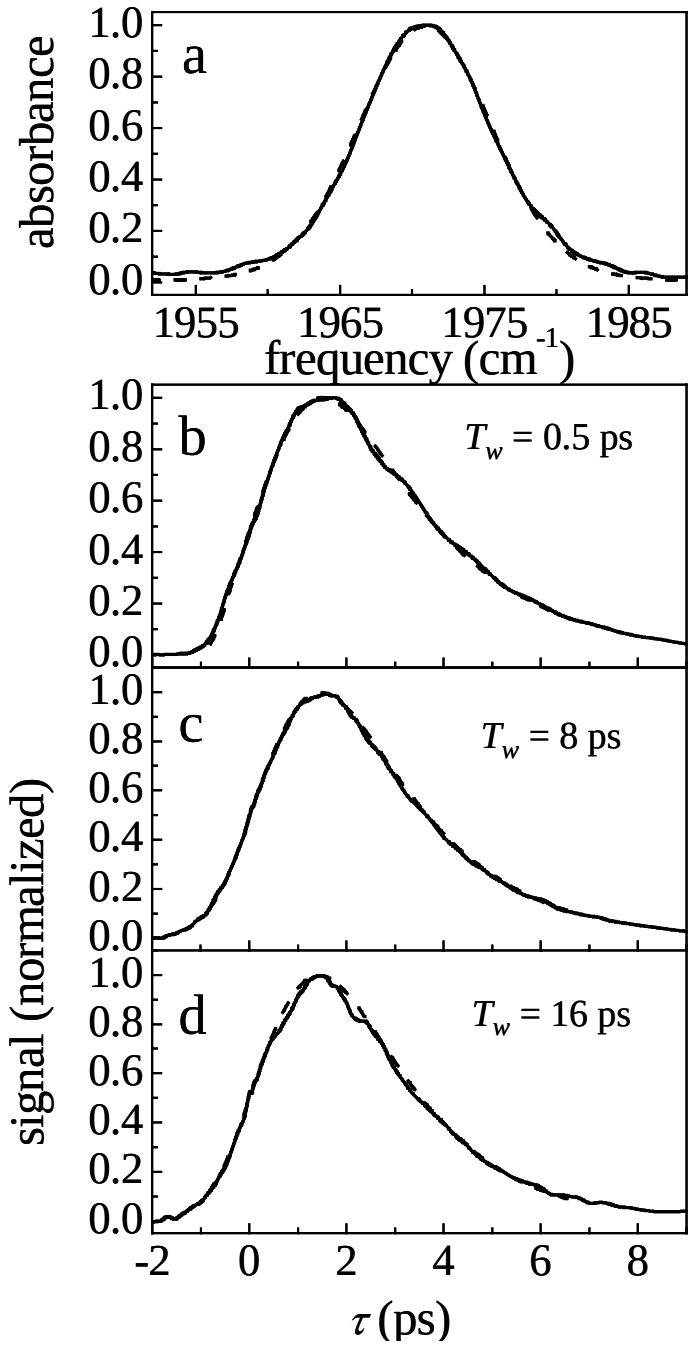

Figure S3. Experimental linear spectrum (a) and vibrational echo decay data at b) T_w = 0.5 ps, c) 8 ps, and d) 16 ps (solid lines) overlaid with the best fit linear specrum and vibrational echo decays calculated from nonlinear response theory (dashed lines) for H64V in trehalose at 1971 cm^{-1}.

Best fit *C*(*t*) parameters

	Δ_0 (rad/ps)	Δ_1 (rad/ps)	τ_1 (ps)	Δ_2 (rad/ps)	τ_2 (ps)
HbCO aqueous (CIII)	0.43	1.05	0.18	0.44	8.4
HbCO trehalose (CIII)	0.89	1.21	0.09	0.11	20.0
H64V aqueous	0.56	1.05	0.12	0.37	5.1
H64V trehalose	0.81	0.97	0.08	0.14	28.0
***Ht*-M61A aqueous**	0.92	1.05	0.11	0.65	2.3
***Ht*-M61A trehalose**	1.14	1.01	0.11	0.19	26.7

Table S1. Best fit *C*(*t*) parameters (see Eq. (1)) for the three proteins in this study. These values simultaneously reproduce the experimentally measured linear infrared spectra and the vibrational echo decays at several T_w delay times.

Aqueous H64V simulations

A comparison between the calculated and fitted FFCFs for H64V in aqueous solution and their corresponding vibrational echo signals has been discussed elsewhere.[7] It is notable that both calculated and experimental correlation functions for H64V in an aqueous environment are characterized by a subpicosecond motionally-narrowed regime, followed by slower dynamics. However, they differ in the nature of the decay following the motionally-narrowed regime. The experimental $C(t)$ contains a static term, which is necessary to reproduce the linear absorption spectrum, while the computed $C(t)$ decays nearly to zero on a time scale of 50 ps. It is notable that the magnitude of the fitted and calculated $C(0)$s for H64V are in fact within 38 and 44% of each other for the aqueous and trehalose environments, respectively.[7]

References

(1) Finkelstein, I. J.; McClain, B. L.; Fayer, M. D. *J. Chem. Phys.* **2004**, *121*, 877-885.

(2) Rector, K. D.; Engholm, J. R.; Rella, C. W.; Hill, J. R.; Dlott, D. D.; Fayer, M. D. *J. Phys. Chem. A.* **1999**, *103*, 2381-2387.

(3) Rector, K. D.; Jiang, J.; Berg, M.; Fayer, M. D. *J. Phys. Chem. B* **2001**, *105*, 1081-1092.

(4) Mayer, E. *J. Am. Chem. Soc* **1994**, *116*, 10571-10577.

(5) Merchant, K. A.; Thompson, D. E.; Fayer, M. D. *Phys. Rev. A* **2002**, *65*, 023817.

(6) Park, E. S.; Boxer, S. G. *J. Phys. Chem. B* **2002**, *106*, 5800-5806.

(7) Finkelstein, I. J.; Goj, A.; McClain, B. L.; Massari, A. M.; Merchant, K. A.; Loring, R. F.; Fayer, M. D. *J. Phys. Chem. B* **2005**, (submitted).

(8) Hayashi, T.; Jansen, T. l. C.; Zhuang, W.; Mukamel, S. *J. Phys. Chem. A* **2005**, *109*, 64-82.

(9) Kwac, K.; Cho, M. *J. Chem. Phys.* **2003**, *119*, 2247-2255.

(10) Moller, K.; Rey, R.; Hynes, J. *J. Phys. Chem. A* **2004**, *108*, 1275-1289.

(11) Schmidt, J.; Corcelli, S.; Skinner, J. *J. Chem. Phys.* **2004**, *121*, 8887-8896.

(12) Merchant, K. A.; Noid, W. G.; Akiyama, R.; Finkelstein, I. J.; Goun, A.; McClain, B. L.; Loring, R. F.; Fayer, M. D. *J. Am. Chem. Soc.* **2003**, *125*, 13804-13818.

(13) Potter, W. T.; Hazzard, J. H.; Choc, M. G.; Tucker, M. P.; Caughey, W. S. *Biochemistry* **1990**, *29*, 6283-6295.

(14) Janes, S. M.; Dalickas, G. A.; Eaton, W. A.; Hochstrasser, R. M. *Biophys. J.* **1988**, *54*, 545.

(15) Merchant, K. A.; Thompson, D. E.; Fayer, M. D. *Phys. Rev. Lett.* **2001**, *86*, 3899-3902.

(16) McClain, B. L.; Finkelstein, I. J.; Fayer, M. D. *J. Am. Chem. Soc* **2004**, *126*, 15702-15710.

(17) McClain, B. L.; Finkelstein, I. J.; Fayer, M. D. *Chem. Phys. Lett.* **2004**, *392*, 324-329.